Reversible Triclinic-Rhombohedral Phase Transition in $LiHf_2(PO_4)_3$: Crystal Structures from Neutron Powder Diffraction

Enrique R. Losilla, Miguel A. G. Aranda, María Martínez-Lara, and Sebastián Bruque*

Departamento de Química Inorgánica, Cristalografía y Mineralogía, Universidad de Málaga, Aptd. 59, 29071 Málaga, Spain

Received February 7, 1997. Revised Manuscript Received April 11, 1997[⊗]

Crystalline single-phase $LiHf_2(PO_4)_3$ has been synthesized. It shows a phase transition at 235 K that has been characterized through DSC, low-temperature X-ray diffractometry, and ionic conductivity measurements. The crystal structures of the two phases have been established by neutron powder diffraction at 175 and 320 K. The room-temperature phase is rhombohedral $R\bar{3}c$, $Z = 6$, $a = 8.8306(1)$ Å and $c = 22.0270(5)$ Å and the structure has been refined by the Rietveld method to $R_{wp} = 6.29\%$ and $R_F = 4.68\%$. The framework is similar to that shown by NASICON materials with the Li cations disordered out of the M1 position and close to the M1−M2 bottleneck site. The crystallographically refined composition was $Li_{0.87}Hf_{2.032}(PO_4)_3$ in agreement with the chemical analysis. The low-temperature phase is triclinic C1, $Z = 4$, $a = 15.2680(4)$ Å, $b = 8.6946(3)$, $c = 9.0722(2)$ Å, $\alpha = 89.323(2)°$, $\beta = 123.740(2)°$, and $\gamma = 90.666(2)°$, and the structure has been refined to $R_{wp} = 4.61\%$ and $R_F = 2.25\%$. This is a common reversible order−disorder phase transition with some subtle structural changes. These structural changes and the consequences in the ionic conductivity properties will be discussed. This is the first structural report on a low-temperature phase in the Li−NASICON system.

Introduction

The discovery of NASICON (the acronym for Na superionic conductor) materials[1,2] was an important development in the solid electrolytes field as it provided a three-dimensional network that encloses channels where superionic conductivity may occur. In the NASICON type structure, the negatively charged framework $[M_2(XO_4)_3]$ consists of MO_6 octahedra surrounded by six XO_4 tetrahedra and of XO_4 tetrahedra surrounded by four MO_6 octahedra. This framework results in channels where the adequate amount of compensating cations, A, are located. As the oxygen sites are generally fully occupied, the amount of cations in the channels depends upon the oxidation state of the M and X atoms. This open framework allows the researcher to play with the cations in the A, M, and X sites giving rise to a vast quantity of stoichiometries. The first report on NASICON materials dealt with $NaZr_2(PO_4)_3$ (space group $R\bar{3}c$, $a_r = 8.82$ Å, and $c_r = 22.75$ Å) and the solid solution $Na_{1+x}Zr_2P_{3-x}Si_xO_{12}$, crystallographic data for $Na_3Zr_2PSi_2O_{12}$ (space group $C2/c$, $a = 15.59$ Å, $b = 9.03$ Å, $c = 9.21$ Å, $\beta = 123.7°$), with the following relationship between these cells: $a_m = 2a_r \sin 60$, $b_m = a_r$, $c_m = c_r/3\cos(\beta - 90)$.[2]

On the other hand, Li cells have a very important market due to their unmatchable properties of high potential ($E°_{red} = -3.024$ V), very lightweight and, hence, very high energy-density storage properties. There is an intense research effort in three-dimensional Li-based solid electrolytes for all solid lithium batteries. NASICON type materials with Li cations in the channels are promising candidates as electrolytes in these cells if the conductivity properties at room temperature are enhanced.

Many reports have been published dealing with Li−NASICON materials. In general, the properties of the studied compounds strongly depend upon the chemical stoichiometry and the thermal treatment. At this point it is necessary to underline the differences between a nominal "starting" composition, for example, $LiM^{IV}_2(PO_4)_3$, and the final composition of the sample. Li is a volatile cation, and if the temperature to get a single phase has to be increased above 1000 °C, then Li and P_2O_5 may be released. A phase transition between a low-temperature low-symmetry phase and a high-temperature rhombohedral phase has been reported (for M = Ti, Zr, Hf, and Sn) approximately at room temperature. Slight differences in the stoichiometry and, consequently, in the stable phase at room temperature may explain different properties or some contradictory reports on materials with the same nominal composition.

$LiZr_2(PO_4)_3$ shows a first-order phase transition just above room temperature, 25−60 °C.[3] The conductivity is quite poor at room temperature, $\sigma \approx 10^{-9}$ S·cm^{-1}, and increases after the phase transition to $\sigma = 5 \times 10^{-4}$ S·cm^{-1} at 350 °C. Three years later, the same authors[4] increased the reported value of the conductivity of a sample with the same nominal composition to $\sigma = 1.2$

[⊗] Abstract published in *Advance ACS Abstracts,* June 1, 1997.

(1) Goodenough, J. B.; Hong, H. Y.-P.; Kafalas, J. A. *Mater. Res. Bull.* **1976**, *11*, 203−220.
(2) Hong, H. Y.-P. *Mater. Res. Bull.* **1976**, *11*, 173−182.
(3) Petit, D.; Colomban, Ph.; Collin, G.; Boilot, J. P. *Mater. Res. Bull.* **1986**, *21*, 365−371.
(4) Sudreau, F.; Petit, D.; Boilot, J. P. *J. Solid State Chem.* **1989**, *83*, 78−90.

S0897-4756(97)00078-1 CCC: $14.00

$\times 10^{-2}$ S·cm^{-1} at 300 °C. These discrepancies may be due to a better sintering prior to the conductivity measurement or to a slightly different composition of the final sample. On the basis of variable-temperature MAS NMR studies a $R\bar{3}c \rightarrow Cc$ phase transition on cooling was proposed.[4,5] Unfortunately, the crystal structure of this *Cc* monoclinic sample has not yet been established. A single crystal study has been reported in this system.[3] The data were collected at 30 °C and analyzed in the $R\bar{3}c$ space group. The framework was similar to that reported[2] for NASICON materials and the lithium cations were located in the M1 site (0 0 0; 6b position) fully occupied, leaving the M2 site (0.63 0 $^1/_4$; 18e position) completely empty. Although the *R* factor was good, 3.76%, the reported Li position leads to six equivalent Li−O bonds distances of 2.499 Å. This is a quite surprising result as the sum of the effective ionic radii of Li and O gives 2.16 Å for a 6-fold coordination of oxygens.[6] Moreover, bond valence calculations[7,8] with the reported Li−O bond distances yields a valence of 0.37 for the lithium cations. This is too far from 1.00 and clearly indicates that the center of M1 site (000) is not a stable position for Li in this system as it results in too long Li−O bonds.

A comparative ionic conductivity study[9] of $LiM_2(PO_4)_3$ (M = Ti, Zr, Hf) showed phase transitions in the three cases with temperatures of 25, 45, and −18 °C, respectively. The room-temperature conductivities were $\sigma \approx 4 \times 10^{-7}$ S·cm^{-1} for Ti, $\sigma \approx 5 \times 10^{-8}$ S·cm^{-1} for Zr and $\sigma \approx 3 \times 10^{-5}$ S·cm^{-1} for Hf. This last sample showed a better ionic conductivity probably because at room temperature it is the only one that presents a rhombohedral structure. This is supported by the fact that the ionic conductivity of $LiZr_2(PO_4)_3$ at 54 °C, just above the phase transition (rhombohedral structure), is 8×10^{-5} S·cm^{-1}, a jump of 2 orders of magnitude in approximately 25 °C.

For samples with the starting nominal composition $LiHf_2(PO_4)_3$, a study[10] showed two different patterns depending upon the final heating temperature. At 1220 °C, a clean pattern was obtained that can be indexed in the $R\bar{3}c$ space group. However, at 1120 °C a complex pattern was obtained, and the authors suggested a primitive-monoclinic space group although the corresponding unit-cell parameters were not reported. A close inspection of this pattern (Figure 1a of ref 10) suggests that unreactive products such as HfP_2O_7 may be present. This clearly shows that very much care has to be taken in the different synthesis steps if a single phase is wanted.

$LiTi_2(PO_4)_3$ is probably the most studied Li−NASICON system. The smaller size of the Ti^{4+} cations makes the size of the sites in the channels more appropriate for lithium cations. A neutron powder diffraction[11] was carried out in a related system $Li_{1+x}Ti_{2-x}In_x(PO_4)_3$, for $x = 0.12$ and 0.15. The symmetry of these samples was $R\bar{3}c$ and Li cations were located in the M1 site (0 0 0), 97(4)%, and the rest in the M2 site (−0.30 0 $^1/_4$), 5(2)%. Lithium may be intercalated electrochemically[12] to yield $Li_3Ti_2(PO_4)_3$. The conductivity may be increased by partial substitution of Ti^{4+} by trivalent cations as Al, Ga, In, Ti, Sc, Y, La, Cr, Fe, mainly due to a much lower porosity of the pellets.[13−15] An alternative way to improve the conductivity properties is to mix $LiTi_2(PO_4)_3$ with lithium salts.[16,17]

$LiSn_2(PO_4)_3$ has also been reported. A reversible phase transition between a low-temperature, possibly monoclinic *Cc* phase, and a high-temperature rhombohedral $R\bar{3}c$ phase occurs with hysteresis.[18,19] Unfortunately, although this transition has been studied by variable-temperature diffractometry, MAS NMR and DSC, the crystal structure of the low-temperature phase has not been reported so far.

Finally, the crystal structure of $LiGe_2(PO_4)_3$ has been studied at room temperature by single-crystal X-ray diffraction and between 300 and 1000 K by neutron powder diffraction.[20] The structure is rhombohedral, $R\bar{3}c$, in all studied temperatures and the thermal expansion was reported. The lithium atoms are located in the M1 site, and they are slightly disordered out to the (0.025 0 0) position, resulting in an average Li−O bond distance of 2.21 Å.

In this paper we report the synthesis and the structural characterization of $LiHf_2(PO_4)_3$. This material undergoes a phase transition that has been characterized through DSC, low-temperature X-ray diffractometry, and electrical measurements. Two neutron powder diffraction patterns, just above and below the phase transition, have allowed us to establish the crystal structures. For the first time, the structure of a low-temperature phase in the Li−NASICON system has been unraveled.

Experimental Section

Synthesis. Stoichiometric amounts of Li_2CO_3, HfO_2, and $(NH_4)_2HPO_4$ were thoroughly mixed and heated, in steps, up to 1373 K. The reaction was followed by X-ray powder diffraction at the different heating temperatures. The overall reaction is

$$^1/_2Li_2CO_3 + 2HfO_2 + 3(NH_4)_2HPO_4 \xrightarrow{\Delta} LiHf_2(PO_4)_3 + {}^1/_2CO_2 + 6NH_3 + {}^9/_2H_2O$$

The initial mixture was grounded with acetone for 1 h in an agate mortar and heated at 673 K for 1 day, which results in the release out of NH_3, H_2O, and CO_2 gases. At this stage,

(5) Sanz, J.; Rojo, J. M.; Jiménez, R.; Iglesias, J. E.; Alamo, J. *Solid State Ionics* **1993**, *62*, 287−292.
(6) Shannon, R. D. *Acta Crystallogr.* **1976**, *A32*, 751−767.
(7) Altermatt, D.; Brown, I. D. *Acta Crystallogr.* **1985**, *B41*, 240−244.
(8) Brown, I. D.; Altermatt, D. *Acta Crystallogr.* **1985**, *B41*, 244−247.
(9) Kuwano, J.; Sato, N.; Kato, M.; Takano, K. *Solid State Ionics* **1994**, *70/71*, 332−336.
(10) Aono, H.; Sugimoto, E.; Sadaoka, Y.; Imanaka, N.; Adachi, G. *Solid State Ionics* **1993**, *62*, 309−316.
(11) Tran-Qui, D.; Hamdoune, S.; Soubeyroux, J. L.; Prince, E. *J. Solid State Chem.* **1988**, *72*, 309−315.
(12) Delmas, C.; Nadiri, A.; Soubeyroux, J. L. *Solid State Ionics* **1988**, *28/30*, 419−423.
(13) Subramanian, M. A.; Subramanian, R.; Clearfield, A. *Solid State Ionics* **1986**, *18/19*, 562−569.
(14) Aono, H.; Sugimoto, E.; Sadaoka, Y.; Imanaka, N.; Adachi, G. *J. Electrochem. Soc.* **1990**, *137*, 1023−1027.
(15) Ado, K.; Saito, Y.; Asai, T.; Kageyama, H.; Nakamura, O. *Solid State Ionics* **1992**, *53/56*, 723−727.
(16) Aono, H.; Sugimoto, E.; Sadaoka, Y.; Imanaka, N.; Adachi, G. *Chem. Lett.* **1990**, 331−334.
(17) Aono, H.; Sugimoto, E.; Sadaoka, Y.; Imanaka, N.; Adachi, G. *J. Electrochem. Soc.* **1993**, *140*, 1827−1833.
(18) Angenault, J.; Couturier, J. C.; Souron, J. P.; Siliqi, D.; Quarton, M. *J. Mater. Sci. Lett.* **1992**, *11*, 1705−1707.
(19) Martínez-Juarez, A.; Rojo, J. M.; Iglesias, J. E.; Sanz, J. *Chem. Mater.* **1995**, *7*, 1857−1862.
(20) Alami, M.; Brochu, R.; Soubeyroux, J. L.; Gravereau, P.; Flem, G. L.; Hagenmuller, P. *J. Solid State Chem.* **1991**, *90*, 185−193.

if the temperature is increased very rapidly, a very unreactive product, HfP_2O_7, is mainly obtained. To minimize the formation of this product, a heating rate of 0.5 K·min^{-1} was used. To homogenize the sample, intermediate regrindings each 150 °C were carried out. When the reaction mixture reached the temperature, this was held fixed for 1 day before the next heating cycle, up to 1273 K. Finally, the sample was kept at 1273 K for 2 days and at 1373 K for 4 days.

Chemical Analysis. The sample (≈50 mg) was dissolved in concentrated HF acid at ≈60 °C. Lithium content was determined by emission atomic spectroscopy in an air/acetylene flame. K was added, K/Li ratio: 1000/1, to avoid lithium ionization. The experimental lithium content of the sample was 0.98%. The calculated Lithium amount for $LiHf_2(PO_4)_3$ is 1.07%.

X-ray Powder Diffraction Characterization. X-ray powder diffraction data at room temperature were collected on a Siemens D-501 automated diffractometer using graphite-monochromated Cu Kα radiation. The low-temperature X-ray diffraction study was carried out on a Philips PW 1050 diffractometer. A vacuum system (≈10^{-2} bar) avoids the condensation of water. The holder is cooled by a liquid nitrogen flux, and the sample/holder temperature is controlled by the power dissipated by an electrical internal resistance. This system allows control of the temperature with a precision of ±1 °C. The patterns were collected between 173 and 298 K.

Thermal Study. The low-temperature thermal characterization (170−400 K) was carried out on a differential scanning calorimeter Shimadzu DSC-50 equipped with a low-temperature chamber LC-50. The system is cooled by liquid nitrogen, and the sensitivity limit is 0.01 mW. The sample (≈50 mg) was heated/cooled at a rate of 10 K·min^{-1}. The high-temperature thermal characterization (300−1373 K, TGA and DTA) was carried out in air on a Rigaku Thermoflex apparatus at a heating rate of l0 K·min^{-1} with calcined Al_2O_3 as reference.

Neutron Powder Diffraction. Neutron patterns were recorded on D1A diffractometer at ILL neutron source. The $LiHf_2(PO_4)_3$ sample was loaded in a cylindrical vanadium can and mounted in an ILL standard orange cryostat. Two patterns were collected at temperatures of 175 and 320 K, counting for a day for each diffractogram. At the given temperatures, the data collection was delayed for 1 h to allow the phase transition to take place. The experimental conditions were as follows: wavelength, 1.909 Å; useful 2Θ range 12−150°, step size 0.05° (in 2Θ). The data were fitted by the Rietveld method[21] using the GSAS suite of programs.[22] The pseudo-Voigt function[23] corrected for asymmetry[24] at low angles was used to simulate the peak shape for both set of patterns. The scattering lengths, *b*, used in the refinements were 0.007 70 Å for Hf, 0.005 81 Å for O, 0.005 23 Å for P, and −0.002 14 Å for Li.

Ionic Conductivity Characterization. The $LiHf_2(PO_4)_3$ pellet (≈10 × 2 mm) was obtained by applying a uniaxial pressure of 200 MPa (2 tons·cm^{-2}) and heated slowly to the temperature synthesis for good sintering. Platinum lac was deposited onto opposite faces of the pellets and dried by heating at 473 K. The ionic conductivity data were collected with a Hewlett-Packard 4284A impedance analyzer. The pellet, in air, was studied in the temperature range 170−870 K with a ddp of 0.1 V and a frequency range of 20 Hz to 1 MHz.

Results

The room-temperature X-ray powder diffraction study shows that the samples prepared above 1273 K are very crystalline single phases with rhombohedral structure. The unit-cell parameters for the final sample, $LiHf_2(PO_4)_3$, are $a = 8.808$ Å and $c = 21.988$ Å. The samples obtained by heating at temperatures below 1273 K showed diffraction peaks corresponding to HfP_2O_7.

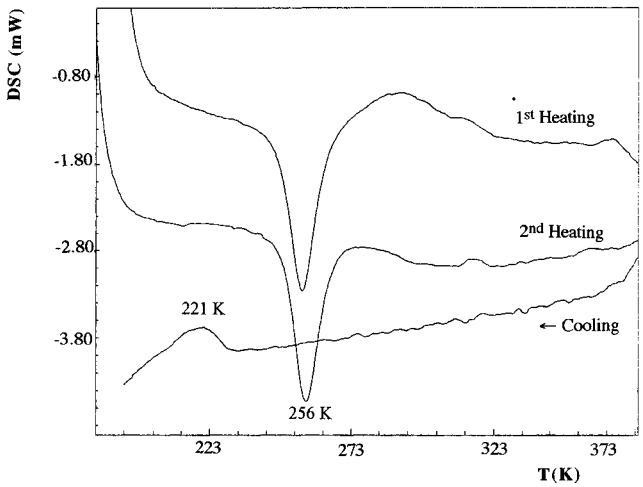

Figure 1. Low-temperature DSC curves for "$LiHf_2(PO_4)_3$". The sample was cooled to 170 K and heated continuously to 400 K (heating curve), followed by a cooling process (cooling curve) to 170 K.

The sample is completely stable at high temperatures, and the thermal study does not show any weight loss or structural transition between room temperature and 1373 K. However, as reported previously,[9] a low-temperature phase transition is evident in the DSC curves (Figure 1). On heating, the phase transition is clearly observed as a sharp endotherm centered at 256 K. This phase transition is reversible and, on cooling, is evident as a broad exotherm centered approximately at 221 K. From these temperature dynamic values, a transition temperature around 235 K can be inferred.

The low-temperature X-ray diffraction study is shown in Figure 2. The phase transition is clearly observed as splitting of many diffraction peaks at temperatures below 250 K. In these conditions, the transition is completely finished at 220 K. Unfortunately, the 173 K pattern that had good statistics to index the low-temperature phase showed extra peaks, probably due to water condensation in the system.

With these results, a neutron diffraction study has been carried out to determine the crystal structure of both phases. The room-temperature $R\bar{3}c$ structure of $LiHf_2(PO_4)_3$ was refined by the Rietveld method using the framework of $NaZr_2(PO_4)_3$ as starting model.[2] First, we refined the overall parameters: histogram scale factor, background parameters, zero shift error, unit-cell parameters, and peak shape parameters for the pseudo-Voigt function. Second, the atomic parameters, positional coefficients, and isotropic temperature factors were refined. At this stage, the lithium cations were positioned at the center of the M1 cavity, 6b special position, (0 0 0). The refinement does not converge, as if the occupation factor is fixed to 1.00, the isotropic temperature factor, U_{iso}, diverges to a value greater than 0.4 Å^2. Alternatively, if the temperature factor is fixed to a reasonable value, 0.03 Å^2, the occupation factor decreases to a value lower than 0.3. Lithium atoms at the M2 sites (18e special position, (0.63 0 1/4)) also does not lead to a stable refinement. Hence, some disordered

(21) (a) Rietveld, H. M. *J. Appl. Crystallogr.* **1969**, *2*, 65−71. (b) Young, R. A., Ed. *The Rietveld Method;* Oxford University Press: Oxford, 1993.

(22) Larson, A. C., von Dreele, R. B. *Program version: PC, summer 96, Los Alamos National Lab. Rep.*, No. LA-UR-86-748, 1987.

(23) Thompson, P.; Cox, D. E.; Hasting, J. B. *J. Appl. Crystallogr.* **1987**, *20*, 79−83.

(24) Finger, L. W.; Cox, D. E.; Jephcoat, A. P. *J. Appl. Crystallogr.* **1994**, *27*, 892−900.

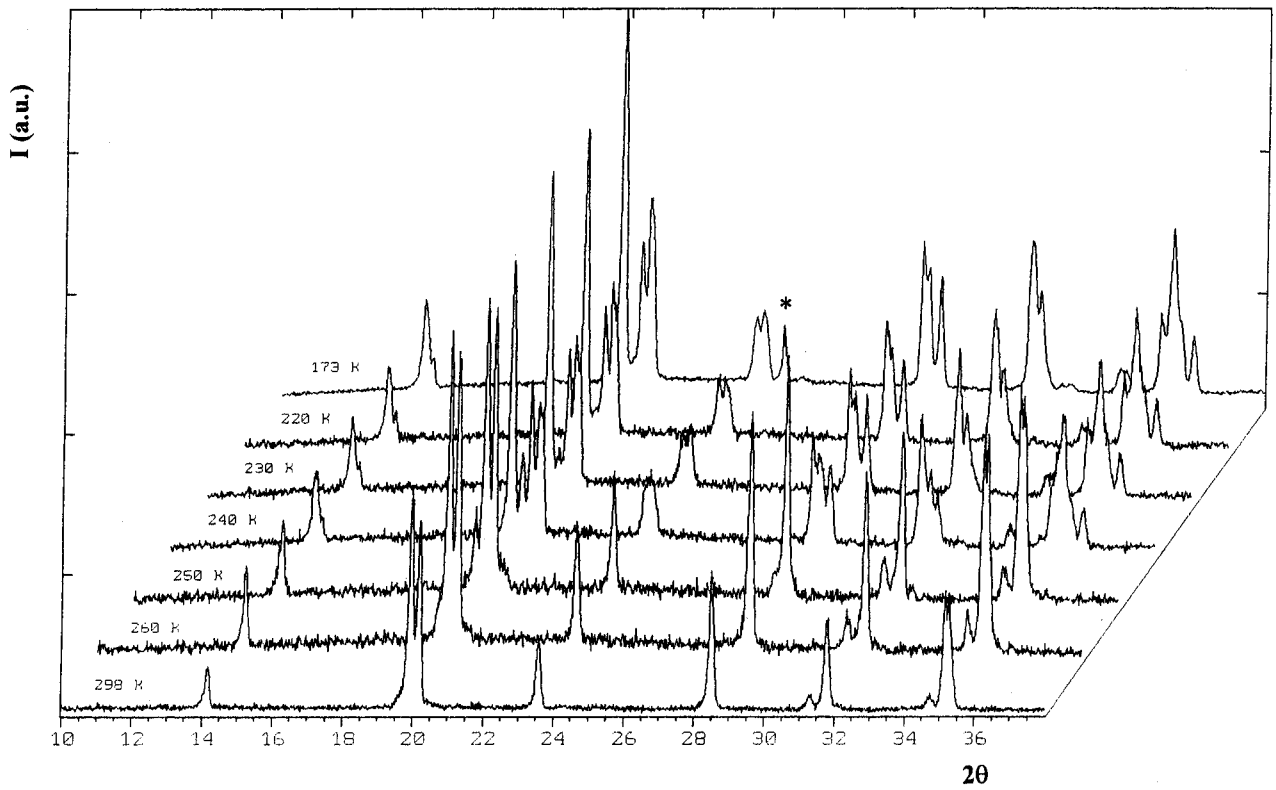

Figure 2. Partial low-temperature X-ray diffraction patterns for "$LiHf_2(PO_4)_3$". The diffractogram at 173 K has more counting time showing a better signal-to-noise ratio, and the peak marked * is due to the sample environment.

Table 1. Structural Parameters for $Li_{0.87}Hf_{2.032}(PO_4)_3$ at 320 K in Space Group *R*3*c*

atom	*x*	*y*	*z*	fract	U_{iso}/Å^2
Hf	0.00	0.00	0.1421(1)	1.00	0.0024(6)
P	0.2876(3)	0.00	0.25	1.00	0.0042(7)
O(1)	0.1851(3)	−0.0102(3)	0.1936(1)	1.00	0.0157(5)
O(2)	0.1947(2)	0.1701(2)	0.0841(1)	1.00	0.0107(5)
Li	−0.135(4)	0.043(5)	0.006(2)	0.145(5)	0.018(9)
Hf(b)	0.00	0.00	0.25	0.032(−)	0.018(−)

models were tested. A refinement disordering the Li cations out of the M1 center in the (0 0 *z*) special position (along the high-symmetry axis) did not converge. Then, Li was placed at the M1 site but disordered out in a test general position 36f (0.02 0.02 0.01), occupation factor $^1/_6$, and allowing to vary slowly. In these conditions, the refinement converged smoothly.

The lithium deficit found from chemical analysis (0.09% w/w) suggests a nonstoichiometric sample with ≈14% of lithium sites deficiency. As the occupation factors of the framework atoms converged to full occupancy, some tests were carried out to find the Hf needed to balance the charges. The excess of Hf^{4+} (≈1.5 % per formula) was refined in the (0 0 $^1/_4$) position. Finally, the isotropic temperature factors of Li and Hf(b) was constrained to be the same and the occupation factors in such a way to ensure electroneutrality. In these conditions, the crystallographically refined stoichiometry is $Li_{0.87(3)}Hf_{2.032(7)}(PO_4)_3$.

The final refinement (space group $R\bar{3}c$, $Z = 6$, $a = 8.8306(1)$ Å, $c = 22.0270(5)$ Å, and $V = 1487.54(6)$ Å^3) converged to $R_{WP} = 6.29\%$, $R_P = 5.12\%$, and $R_F = 4.68\%$, with the atomic parameters given in Table 1. The fit to the 320 K neutron pattern is shown in Figure 3. The bond angles and distances are given in Table 2.

The 175 K neutron pattern for $LiHf_2(PO_4)_3$ is very complex, but the reversibility of the phase transition indicates a subtle structural change. Initially, we tried to explain the 175 K pattern with a monoclinic distortion, *C*2/*c*, like that shown by $Na_{1+x}Zr_2P_{3-x}Si_xO_{12}$ at $T \approx 420$ K.[25,26] We used the overall parameters determined for the high-temperature phase, and a monoclinic *C*2/*c* cell with parameters $a \approx 15.1$ Å, $b \approx 8.7$ Å, $c \approx 9.0$ Å, and $\beta = 123.7°$. Although the coarse features of the pattern could be explained, some small peaks remained unindexed and there was strong differences between the observed and calculated intensities, being reflected in a very high R_{WP} factor, ≈ 22%. Reversible phase segregation was ruled out, and a C-centered monoclinic structure *Cc* does not index all the peaks. Additionally, some time-consuming tests with primitive monoclinic cells were explored without success.

At this stage, and using the framework of $Na_3Zr_2PSi_2O_{12}$ as starting model,[2] we developed a related triclinic framework structure lowering in symmetry from *C*2/*c* to $C\bar{1}$. As this triclinic structure has many atomic parameters to refine, soft constraints in the three crystallographically independent PO_4 tetrahedra (P−O bond distances 1.53(2) Å, and O···O distances 2.55 Å) were imposed in the initial phase of the refinement to avoid the structure blowing up when all parameters start to vary. The refinement of the framework converged quickly and R_{wp} fell from 22% to 6%. The soft constraints were completely removed, and all overall and atomic positional parameters were allowed to refine to convergence. Then, the Li cations were located from the more intense peaks in the difference Fourier map and refined, with a fixed occupation factor of 0.86.

(25) Baur, W. H.; Dygas, J. R.; Whitmore, D. H.; Faber, J. *Solid State Ionics* **1986**, *18/19*, 935−943.
(26) Didisheim, J. J.; Prince, E.; Wuensch, B. J. *Solid State Ionics* **1986**, *18/19*, 944−958.

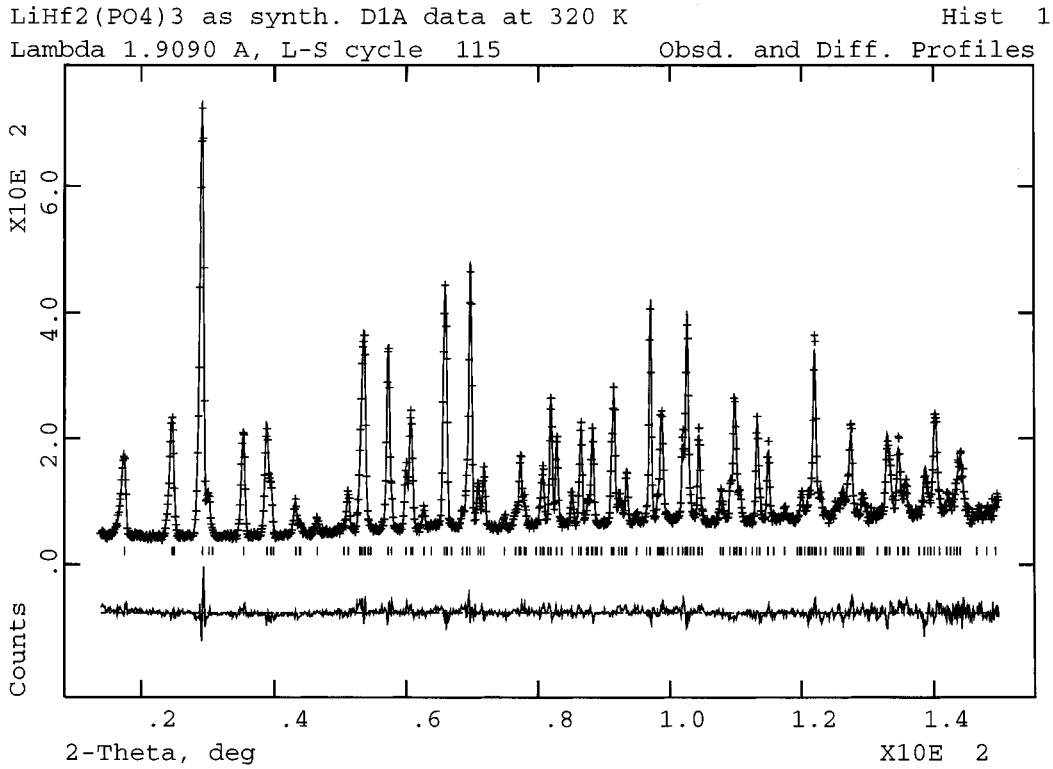

Figure 3. Final observed (crosses), calculated (full line), and difference (bottom) neutrons ($\lambda = 1.909$ Å) profiles for "$LiHf_2(PO_4)_3$" at 320 K. Allowed reflection marks in the R$\bar{3}c$ space group are also shown.

Table 2. Some Bond Distances (Å) and Angles (deg) for "$LiHf_2(PO_4)_3$" at 320 K

Hf−O(1) × 3	2.029(2)	P−O(1) × 2	1.513(2)
Hf−O(2) × 3	2.065(2)	P−O(2) × 2	1.543(3)
Li−O(2)	1.74(4)	Li−O(2)	2.41(3)
Li−O(1)	2.33(4)	Li−O(2)	2.60(4)
O(1)−Hf−O(1) × 3	91.7(1)	O(1)−P−O(1)	110.7(2)
O(1)−Hf−O(2) × 3	89.0(1)	O(1)−P−O(2) × 2	107.5(1)
O(1)−Hf−O(2) × 3	93.5(1)	O(1)−P−O(2) × 2	111.6(1)
O(1)−Hf−O(2) × 3	174.7(1)	O(2)−P−O(2)	108.0(2)
O(2)−Hf−O(2) × 3	85.7(3)		
Hf−O(1)−P	158.2(2)	Hf−O(2)−P	142.3(1)

Due to the complexity of the structure, 18 atoms in general positions, the low temperature of the pattern, and mainly the presence of pseudosymmetry (the structure is pseudomonoclinic and it is also pseudorhombohedral) some temperature factors were negatives. Hence, all temperature factors of the framework atoms were constrained to have the same value. The final refinement (space group $C\bar{1}$, $Z = 4$, $a = 15.2680(4)$ Å, $b = 8.6946(3)$, $c = 9.0722(2)$ Å, $\alpha = 89.323(2)°$, $\beta = 123.740(2)°$, $\gamma = 90.667(2)°$, and $V = 1001.39(4)$ Å^3) converged to $R_{wp} = 4.61\%$, $R_P = 3.69\%$, and $R_F = 2.25\%$. The atomic parameters are given in Table 3. The fit to the 320 K neutron pattern is shown in Figure 4. The bond angles and distances are given in Table 4.

The ionic conductivity for the low-temperature phase is so low that it is barely measurable, as the resistences are so high that could not be obtained with an acceptable precision. However, the conductivity increases very much after the phase transition. It must be underlined that bulk and intergrain components of the resistivity are not sufficiently separated. Hence, the reported conductivity overall values are probably limited by the intergrain component. The overall conductivities at room temperature and 573 K have been estimated as 9.2×10^{-8} and 3.6×10^{-4} S·cm^{-1}, respectively. The crystallographic density of the sample is 4.38 g·cm^{-3} and

Table 3. Structural Parameters for "$LiHf_2(PO_4)_3$" at 175 K in Space Group $C\bar{1}$[a]

atom	*x*	*y*	*z*
Hf(1)	0.1042(6)	0.2427(9)	0.0632(7)
Hf(2)	−0.1088(5)	0.2521(8)	0.4263(8)
P(1)	−0.0018(7)	0.0390(8)	0.2498(12)
P(2)	0.3567(6)	0.1096(8)	0.2580(11)
P(3)	−0.3597(7)	0.1041(9)	0.2579(13)
O(1)	0.1497(5)	0.4346(8)	0.2238(10)
O(2)	−0.1388(6)	0.4361(9)	0.2661(10)
O(3)	0.4317(6)	0.4625(8)	0.0585(10)
O(4)	−0.4371(5)	0.4153(8)	0.3850(10)
O(5)	0.2544(6)	0.1646(8)	0.2368(12)
O(6)	−0.2637(5)	0.1960(9)	0.3100(9)
O(7)	0.3622(6)	0.1705(8)	0.1086(10)
O(8)	−0.3816(5)	0.0953(7)	0.4027(10)
O(9)	0.4481(6)	0.1751(9)	0.4401(11)
O(10)	−0.4530(6)	0.1803(8)	0.0922(11)
O(11)	0.0713(6)	0.1665(8)	0.2536(10)
O(12)	−0.0797(5)	0.1082(8)	0.2832(10)
Li	0.110(2)	0.347(3)	0.419(4)

[a] Framework $U_{iso} = 0.009(4)$ Å^2; Li $U_{iso} = 0.018(6)$ Å^2, Li fract = 0.86.

that obtanied from the mass and volume of the sintered pellet is 2.89 g·cm^{-3}. Hence, the porosity of this pellet was 35%.

To test the influence of lithium deficiency in the ionic conductivity properties, another sample with more Li was measured. This sample was obtained by the reaction of the starting compound with melted $LiNO_3$ at 673 K. After a thoroughly washing, the chemical analysis gave $Li_{0.91}Hf_{2.022}(PO_4)_3$. A pellet of this sample, 34% of porosity, shows better conductivity values, 3.2×10^{-7} S·cm^{-1} at room temperature and 1.1×10^{-3} S·cm^{-1} at 573 K. The Arrhenius plots for both samples are shown in Figure 5. The activation energies for the conduction process, in these rhombohedral phases, have been calculated from the slopes of these lines. The

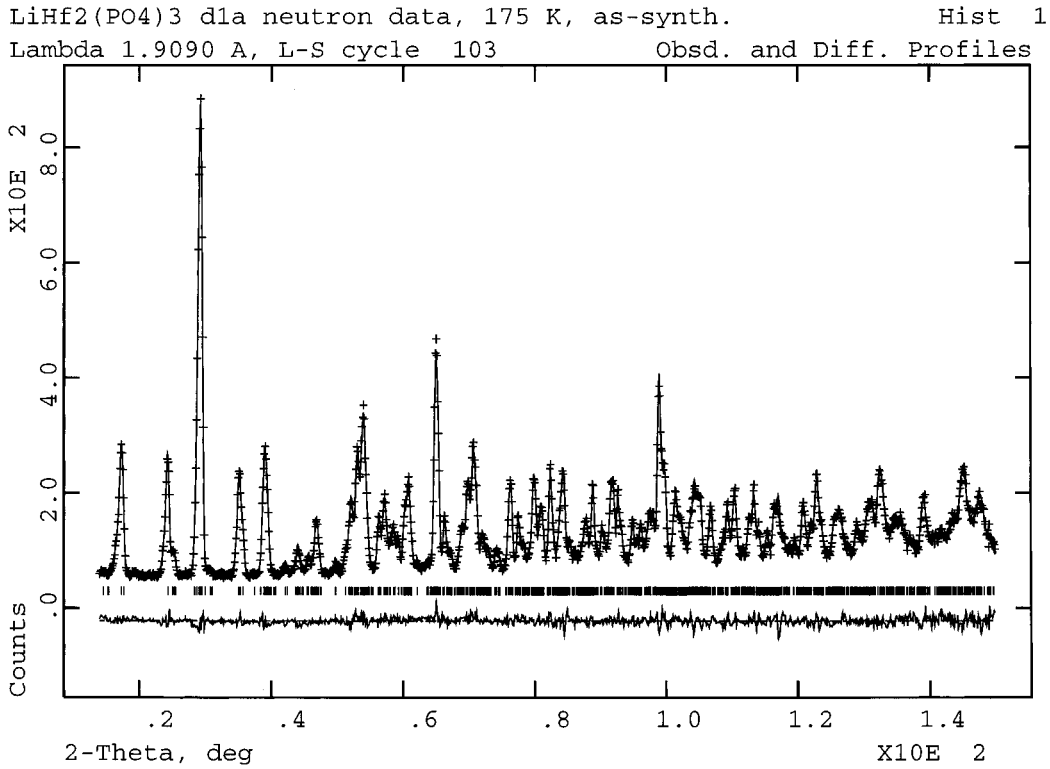

Figure 4. Neutron Rietveld plot for "$LiHf_2(PO_4)_3$" at 175 K, as in Figure 3, showing the allowed reflection marks in the $C\bar{1}$ space group.

Table 4. Bond Distances (Å) and Angles (deg) for "$LiHf_2(PO_4)_3$"at 175 K

Hf(1)−O(1)	2.072(9)	Hf(2)−O(2)	2.025(9)	Li−O(1)	2.285(28)
Hf(1)−O(3)	2.013(9)	Hf(2)−O(4)	2.043(9)	Li−O(5)	2.621(26)
Hf(1)−O(5)	2.050(11)	Hf(2)−O(6)	2.039(9)	Li−O(8)	2.170(25)
Hf(1)−O(7)	2.028(11)	Hf(2)−O(8)	2.121(9)	Li−O(9)	1.929(30)
Hf(1)−O(10)	2.040(10)	Hf(2)−O(9)	2.137(9)	Li−O(11)	2.027(26)
Hf(1)−O(11)	2.145(10)	Hf(2)−O(12)	2.035(10)		
P(1)−O(3)	1.594(11)	P(2)−O(2)	1.510(12)	P(3)−O(1)	1.533(10)
P(1)−O(4)	1.511(11)	P(2)−O(5)	1.545(12)	P(3)−O(6)	1.491(12)
P(1)−O(11)	1.551(11)	P(2)−O(7)	1.495(12)	P(3)−O(8)	1.525(11)
P(1)−O(12)	1.513(12)	P(2)−O(9)	1.563(12)	P(3)−O(10)	1.533(12)
O(3)−P(1)−O(4)	108.5(6)	O(2)−P(2)−O(5)	109.9(7)	O(1)−P(3)−O(6)	112.8(6)
O(3)−P(1)−O(11)	109.7(6)	O(2)−P(2)−O(7)	111.3(6)	O(1)−P(3)−O(8)	103.1(6)
O(3)−P(1)−O(12)	107.2(6)	O(2)−P(2)−O(9)	109.0(6)	O(1)−P(3)−O(10)	111.0(7)
O(4)−P(1)−O(11)	110.2(7)	O(5)−P(2)−O(7)	109.8(6)	O(6)−P(3)−O(8)	113.2(7)
O(4)−P(1)−O(12)	111.1(6)	O(5)−P(2)−O(9)	105.2(7)	O(6)−P(3)−O(10)	107.3(6)
O(11)−P(1)−O(12)	110.0(6)	O(7)−P(2)−O(9)	111.5(6)	O(8)−P(3)−O(10)	109.4(5)
O(1)−Hf(1)−O(3)	171.2(5)	O(2)−Hf(2)−O(4)	172.2(5)	Hf(1)−O(1)−P(3)	152.9(6)
O(1)−Hf(1)−O(5)	86.4(4)	O(2)−Hf(2)−O(6)	94.3(4)	Hf(2)−O(2)−P(2)	143.6(6)
O(1)−Hf(1)−O(7)	96.9(5)	O(2)−Hf(2)−O(8)	87.0(4)	Hf(1)−O(3)−P(1)	142.0(6)
O(1)−Hf(1)−O(10)	91.4(4)	O(2)−Hf(2)−O(9)	84.9(4)	Hf(2)−O(4)−P(1)	161.2(6)
O(1)−Hf(1)−O(11)	79.1(4)	O(2)−Hf(2)−O(12)	94.3(4)	Hf(1)−O(5)−P(2)	145.7(6)
O(3)−Hf(1)−O(5)	88.3(4)	O(4)−Hf(2)−O(6)	91.7(4)	Hf(2)−O(6)−P(3)	160.1(6)
O(3)−Hf(1)−O(7)	90.4(4)	O(4)−Hf(2)−O(8)	88.1(3)	Hf(1)−O(7)−P(2)	170.4(6)
O(3)−Hf(1)−O(10)	93.3(4)	O(4)−Hf(2)−O(9)	88.7(4)	Hf(2)−O(8)−P(3)	138.1(5)
O(3)−Hf(1)−O(11)	93.6(4)	O(4)−Hf(2)−O(12)	89.9(4)	Hf(2)−O(9)−P(2)	140.8(6)
O(5)−Hf(1)−O(7)	93.3(4)	O(6)−Hf(2)−O(8)	89.7(4)	Hf(1)−O(10)−P(3)	154.2(6)
O(5)−Hf(1)−O(10)	175.2(5)	O(6)−Hf(2)−O(9)	175.3(5)	Hf(1)−O(11)−P(1)	132.8(6)
O(5)−Hf(1)−O(11)	86.8(4)	O(6)−Hf(2)−O(12)	97.3(4)	Hf(2)−O(12)−P(1)	149.1(5)
O(7)−Hf(1)−O(10)	91.2(4)	O(8)−Hf(2)−O(9)	85.7(4)		
O(7)−Hf(1)−O(11)	175.2(5)	O(8)−Hf(2)−O(12)	172.8(5)		
O(10)−Hf(1)−O(11)	88.6(4)	O(9)−Hf(2)−O(12)	87.4(4)		

values of E_a are 0.48 eV for a Li content of 86% and 0.47 eV for a Li content of 91%.

Discussion

As shown in the synthetic study and to avoid the formation of unreactive HfP_2O_7, the samples have to be heated slowly to temperatures above 1273 K. In these conditions, highly crystalline single-phase "$LiHf_2(PO_4)_3$" is obtained. However, this high temperature may result in nonstoichiometric samples with Li deficiency. It has to be noted that the contribution of the Li cations to the overall neutron scattering of the sample, $Li_{0.87}Hf_{2.032}(PO_4)_3$, is 1.9%. This small number together with the Li disorder in the structure are the two main factors that give high errors in the refined Li position and composition. The crystallographically refined stoichi-

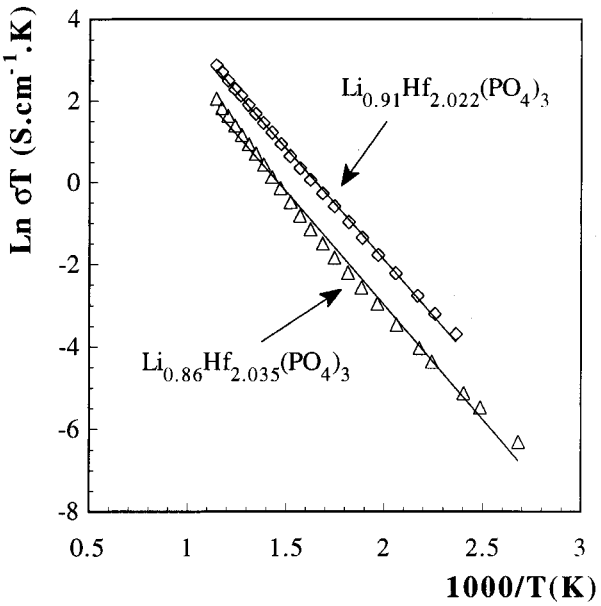

Figure 5. Arrhenius plot of the electrical conductivity for $Li_{0.86}Hf_{2.035}(PO_4)_3$ and $Li_{0.91}Hf_{2.022}(PO_4)_3$.

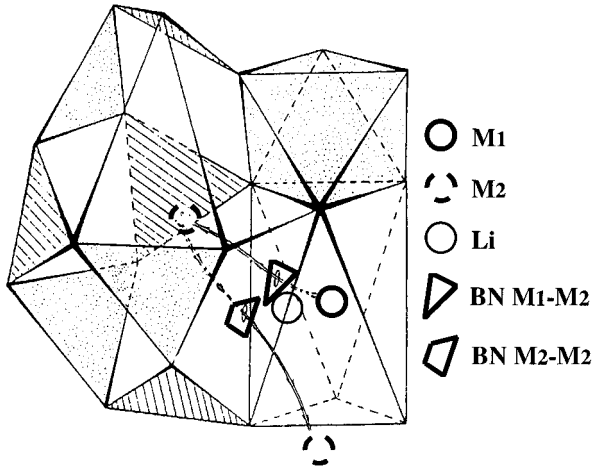

Figure 6. Polyhedra linking in the NASICON R$\bar{3}$*c* type structure. Detailed environments of the M1, M2, M1−M2 bottleneck, M2−M2 bottleneck, and Li position in $LiHf_2(PO_4)_3$ are shown.

ometry, $Li_{0.87(3)}Hf_{2.032(7)}(PO_4)_3$, agrees well with the lithium per formula determined experimentally, 0.86.

The DSC and the low-temperature X-ray diffraction data for $LiHf_2(PO_4)_3$ show a reversible phase transition at approximately 235 K. The high-temperature phase is rhombohedral, and the framework is similar to that of the NASICON materials.[2] The only difference is the Li position. The lithium atoms are located out of the center of the M1 site, at a distance of 1.40 Å. Li atoms are close to the bottleneck site between the M1 and M2 sites (Figure 6). This bottleneck position (−0.14 0.02 −0.013) and those related by symmetry have a possible good oxygens environment for the Li cations. However, if the Li are positioned in this site and refined freely, they converged to the reported position that is 0.5 Å away. One of the Li−O bond distances is too short, 1.74(4) Å, indicating that the lithium atoms have not been located very precisely. If Li is removed, the R_{wp} factor increases only by 0.5%, indicating the expected low contribution of Li in the refinement. The presence of disorder and the low contribution of Li to the overall scattering precludes a better refinement with this medium resolution data. The Li reported position is not unknown in the NASICON materials. For instance, two independent powder neutron diffraction studies for $CuTi_2(PO_4)_3$[27] and $CuZr_2(PO_4)_3$[28] located the Cu(I) cations in a very similar position, for example (0.10 0.06 −0.003) for M = Ti, quite close to the M1−M2 bottleneck and disordered.

The refinement suggests that a slight excess of Hf^{4+} compensates the Li vacancies. Although, the reported Hf(b) position has a good oxygens environment, six at 2.09 Å, there are very short distances to Hf, 2.4 Å, and P, 2.5 Å. Hence, this position must be energetically unstable although it cannot be ruled out completely as local relaxations may allow to accommodate this excess of Hf (≈3% of the site). Including Hf(b) in the refinement improved R_{wp} by 0.1%. Alternatively, the excess of Hf may be situated in the channels and are spatially disordered. The contribution of the excess of Hf to the overall scattering power of the sample is 0.24%, making it difficult to locate it precisely.

The low-temperature structure of $LiHf_2(PO_4)_3$ is triclinic $C\bar{1}$, and the lithium atoms are ordered. It is a complex structure with 18 atoms in the asymmetric part of the unit cell. There are two crystallographically independent HfO_6 octahedra and three PO_4 tetrahedra. This is in agreement with a recent MAS NMR study[29] of a similar sample where three ^{31}P resonances signals are observed below the phase transition. As shown in Table 4, all bond distances and angles are within the normal values. The lithium atoms present a 5-fold coordination of oxygens with four bond distances around 2.0 Å and one long interaction at 2.62 Å. If Li is removed, the R_{wp} factor increases by 0.4%. In this triclinic structure, there are several M1−M2 bottleneck sites as they are not longer equivalent by symmetry. The lithium atoms position refined to (0.110 0.347 0.419), and they are 2.0 Å away from the center of the M1 site ($^1/_4$ $^1/_4$ $^1/_2$) and at a distance of 0.3 Å from the bottleneck site (0.125 0.355 0.420).

It is interesting to point out the differences in the oxygen environment for the M1−M2 bottleneck sites. In the high-temperature phase, this bottleneck is a regular triangular face formed by O(2) atoms (see Figure 6). A cation in this site has three short distances to O(2) of 2.16 Å and one long interaction to O(1) of 2.55 Å. A cation, in the M1−M2 bottleneck site reported above in the low-temperature phase, is surrounded by four oxygens (O1, O8, O9, and O11) with distances ranging between 2.07 and 2.12 Å. Hence, the oxygens environment around the bottleneck site is quite different in the two phases. The framework response to the ordering of the Li on cooling is quite evident in the Hf−O−P bond angles. In the rhombohedral phase there are two angles of 142°and 158°. In the triclinic phase, there are 12 symmetry independent angles with values ranging from 133° to 171°. The relationship between the structures of both phases is displayed in Figure 7, in which it can be seen that no framework bonds were broken in the phase transition. However, there is a tilting of the

(27) McCarron, E. M.; Calabrese, J. C.; Subramanian, M. A. *Mater. Res. Bull.* **1987**, *22*, 1421−1426.
(28) Bussereau, I.; Belkhiria, M. S.; Gravereau, P.; Boireau, A.; Soubeyroux, J. L.; Olazcuaga, R.; Le Flem, G. *Acta Crystallogr.* **1992**, *C48*, 1741−1744.
(29) Paris, M. A.; Martin-Juarez, A.; Rojo, J. M.; Iglesias, J. E.; Sanz, J., submitted to *Chem. Mater.*

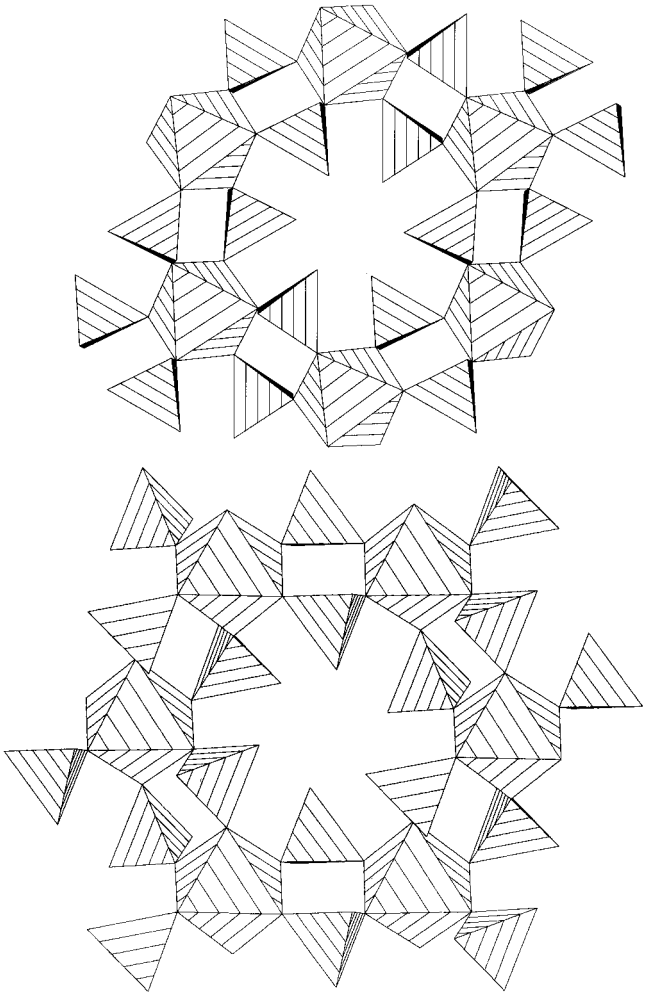

Figure 7. Polyhedral view down the hexagonal *c*-axis of the "$LiHf_2(PO_4)_3$" framework for (top) high- and (bottom) low-temperature phases.

polyhedra to accommodate the lithium cations more efficiently as they order.

This is a reversible and topotactic order−disorder phase transition. The low-temperature phase has low symmetry, $C\bar{1}$, and the lithium cations are ordered. When the temperature increases, a high-temperature, high-symmetry $R\bar{3}c$, phase is formed with the lithium cations disordered in a random way. This Li ordering/disordering affects to the framework that responds with the reported structural change (Figure 7). This transition has important implications to the ionic conductivity properties of the material.

The low-temperature phase is a very poor ionic conductor. Although the Li are localized in a three-dimensional framework with channels, the structure has several different bottleneck positions and some are quite narrow for the Li motion to act properly. However, when the temperature is increased, the lithiums are disordered making the framework rhombohedral with a more appropriate bottleneck for the hopping of the Li cations to take place. The conductivity also depends upon the lithium content. Samples with less lithium deficiencies show higher conductivity. This may be explained as the local relaxations due to the presence of the slight excess of Hf which affect the bottleneck sites. Alternatively, if the excess of Hf^{4+} are situated into the channel, they would act as potential barrier making the Li conductivity more difficult.

We are currently carring out a study relating the Li deficiency, $Li_{1-4x}Hf_{2+x}(PO_4)_3$, with the conductivities and the temperatures of the phase transition that it will be reported elsewhere. To conclude, we would like to suggest that, on the basis of our results, the previously published monoclinic cells for $LiM_2(PO_4)_3$ (M = Zr[4,5] and Sn[18,19]) should be reexamined. The three ^{31}P signals in the MAS NMR for these two samples were explained by a monoclinic *Cc* symmetry, but it may also be taken into account by a triclinic $C\bar{1}$ structure (pseudomonoclinic) as that reported in this study.

Acknowledgment. The work was supported by the research Grant FQM-113 of Junta de Andalucía (Spain). We thank Dr. A. Hewat (ILL) for his help during the neutron diffraction experiment (5-22-455), and to ILL for the provision of neutron facilities. We thank Prof. M. Quarton for many fruitful comments and J. P. Souron and Dr. J. C. Couturier for the help with the low-temperature X-ray study carried out at Laboratoire de Cristallochimie du Solide, Université P. et. M. Curie, Paris. E.R.L. thanks the Junta de Andalucía for a studentship.

CM970078N